ELSEVIER

Cancer Genetics and Cytogenetics 153 (2004) 1–9

Cancer Genetics and Cytogenetics

Lead article

Dissecting karyotypic patterns in renal cell carcinoma: an analysis of the accumulated cytogenetic data

Mattias Höglund[a,*], David Gisselsson[a], Maria Soller[a], Gunnar B. Hansen[a], Peter Elfving[b], Felix Mitelman[a]

[a]*Department of Clinical Genetics, University Hospital, SE-221 85 Lund, Sweden*
[b]*Department of Urology, University Hospital, SE-221 85 Lund, Sweden*

Received 24 November 2003; received in revised form 18 December 2003; accepted 19 December 2003

Abstract Renal cell carcinoma (RCC) is one of the most frequent malignancies in Western societies. The most common subtypes are conventional (clear-cell) and papillary carcinomas, which account for about 75 and 10% of cases, respectively. Cytogenetically, conventional RCC is the best-studied subtype and is characterized by chromosomal losses: loss of the short arm of chromosome 3 being the most common. Papillary tumors frequently show gains of chromosomes 7 and 17, and the more progressed forms have, in addition, gains of chromosomes 16, 12, and 20. In the present investigation we used 796 RCC karyotypes to identify the most frequent genomic imbalances. Tumor cases were then classified with respect to the presence or absence of these imbalances and statistically analyzed to assess the order of appearance of chromosomal imbalances, as well as possible karyotypic pathways and cytogenetic subtypes. We established a temporal order by which the different imbalances occur and showed that at least two cytogenetic pathways exist in RCC, one hypodiploid characterized by presence of 3p− and one hyperdiploid characterized by the presence of +7. The data suggest that conventional-type tumors predominantly evolve through the hypodiploid pathway but that an alternative route may be by hyperdiploidy if 3p− is present. Tumors with a papillary growth pattern predominantly progress through the hyperdiploid pathway. The analyses also revealed three possible cytogenetic subtypes of the papillary tumors, one characterized by the presence of +10, a second by +17 and +3q, and a third by +16, +20, and +12.

1. Introduction

Renal cell carcinoma (RCC) is one of the most frequent malignancies in Western societies and constitutes a heterogeneous group of tumors. Investigations of the underlying development of renal epithelium have identified embryologic correlates of distinct subtypes of RCC, in which genetic alterations seem to be of importance for morphology and tumor growth [1–3]. The most common subtypes of RCC are conventional (clear-cell), papillary, and chromophobe carcinomas, which account for approximately 75, 10, and 5% of malignant kidney tumors, respectively [2]. The most frequent structural change in conventional RCC is loss of genetic material from the short arm of chromosome 3. This may be caused either by terminal deletions, often by breaks extending from 3p13 to 3pter, or by more intricate intrachromosomal rearrangements. Unbalanced translocations are an additional cause for loss of 3p, and translocations with chromosome 5, typically resulting in the der(3)t(3;5)(p13;q22), are particularly frequent. Other chromosomes that often show alterations are chromosomes 6, 8, 9, and 14; chromosome 6 typically shows deletions in the long arm while chromosomes 8, 9, and 14 are frequently lost [3]. Papillary tumors, on the other hand, rarely show deletions of 3p. These tumors are characterized by gains of chromosomes, frequently of chromosomes 7 and 17 only, and of chromosomes 16, 12, and 20 in more progressed forms [4]. The smallest subtype of the three, the chromophobe carcinomas, has been reported to show predominantly losses of whole chromosomes (i.e., loss of chromosomes 1, 2, 6, 10, 13, 17, and 21) [5]. In the present investigation, we have used all cytogenetically aberrant renal cell carcinomas, altogether 796, present in the Mitelman Database of Chromosome Aberrations in Cancer [6] to extract the essential features of the karyotypic evolution of RCC. To identify the most frequent

* Corresponding author. Tel.: +46-46-173739; fax: +46-46-131061.
E-mail address: mattias.hoglund@klingen.lu.se (M. Höglund).

0165-4608/04/$ – see front matter
doi:10.1016/j.cancergencyto.2003.12.019

imbalances we constructed a genomic imbalance map. Tumors were then classified with respect to the presence or absence of these imbalances and analyzed statistically.

2. Materials and methods

2.1. Selection of data

All renal cell carcinomas with abnormal karyotypes were retrieved from the Mitelman Database of Chromosome Aberrations in Cancer [6]. A total of 796 karyotypes were ascertained (November 2002) and used to construct an imbalance map. Based on this map, 28 segments either lost in more than 10% or gained in more than 5% of the cases were identified (Table 1). Each karyotype was then assessed for the presence or absence of the selected imbalances. The number of imbalances per tumor (NIPT) was calculated and the 735 cases with at least one of the selected imbalances were used for further analysis. Subtypes of RCC were identified by consulting the original articles. Cases classified as clear-cell, nonpapillary, or conventional carcinomas were pooled and referred to as conventional carcinomas, chromophilic, and papillary carcinomas pooled and referred to as papillary carcinomas. A total of 230 cases could be classified as conventional carcinomas and 92 as papillary carcinomas. The chromophobe RCC were too few to allow statistical analyses. Information on tumor classification was unclear or absent from the remaining 413 cases. Information on tumor grade was obtained for 267 cases: 81 grade 1, 140 grade 2, and 46 grade 3 cases. In cases where a four-tiered grading system was used, grade 4 was classified as grade 3. Information on tumor stage was available for 242 cases.

2.2. Temporal analysis

The time of occurrence (TO) was determined essentially as described previously [7]. Briefly, all tumors with a given imbalance were selected and the distributions of NIPT were plotted. The modes of these distributions were used as value for TO. To obtain a better estimate of the TO, the selected distributions were resampled with replacement (bootstrapped) 1000 times and the TO was scored after each resampling [8]. The mean of the bootstrapped TO values was then used as the TO for the given imbalance. The bootstrapped 2.5th, 25th, 75th and 97.5th percentiles were also calculated. For the bootstrap estimates, resampling software from Resampling Stats (Arlington, VA) was used.

2.3. Hierarchical cluster analysis and multidimensional scaling

Hierarchical cluster analysis (HCA) and multidimensional scaling (MDS) were performed on distance matrices

Table 1
Frequencies of imbalances in renal cell carcinoma

Imbalances	Abbreviation	RCC (n = 735)	Near-diploid (n = 638)	Polyploid NIPT < 8 (n = 31)	Polyploid NIPT > 7 (n = 66)
+1q11~q44	+1q	8	6	10	24
+2p25-q27	+2	10	7	3	39
+3q12~q29	+3q	11	9	6	27
+5q22~q35	+5q	26	25	19	45
+7p22-q36	+7	42	41	10	67
+8q10~q24	+8q	8	6	6	27
+10p15-q26	+10	7	6	3	12
+12p12-q24	+12	19	16	3	52
+16p13-q24	+16	17	15	0	39
+17p13-q25	+17	17	18	0	20
+19p13-q13	+19	5	2	3	39
+20p13-q13	+20	16	13	3	53
+21p13-q22	+21	6	4	0	20
−1p36~p11	1p−	15	11	29	50
−3p26~p13	3p−	56	54	68	68
−4p15-q35	−4	10	7	13	39
−6q16~q27	6q−	17	13	19	53
−8p23~p10	8p−	21	18	19	52
−9p24-q24	−9	18	15	3	56
−10p15-q26	−10	10	6	3	50
−13p13-q34	−13	13	9	6	56
−14p13-q32	−14	33	29	16	79
−15p13-q26	−15	11	8	0	44
−17p13-q25	−17	12	8	16	42
−18p11-q23	−18	13	9	3	60
−21p13-q22	−21	10	6	3	33
−22p13-q23	−22	10	7	6	38
−Xp22-q28	−X	11	8	6	36

on the basis of Euclidean distances produced by using the imbalances as variables and the tumors as observations. HCA groups objects into clusters and then organizes the clusters into a hierarchical tree according to similarities [9]. A consequence of HCA is that one object may only be part of one cluster. Ward's method was used for cluster formation (http://www.stasoft.com). MDS organizes a higher-dimensional distance matrix in a lower dimensional space to maintain as much as possible of the original distances and, hence, MDS extracts the major features of a distance matrix [9]. HCA and MDS were performed using the Statistica software package (Statsoft, Tulsa, OH).

2.4. Principal component analysis

To search for possible patterns of correlations between the imbalances, principal component analysis (PCA) was performed using the Statistica software package (Statsoft). PCA is a standard multivariate method frequently used to search for underlying structures in data sets [7,10]. In short, principal components are linear combinations of the original variables, orthogonal, and ordered with respect to their variance so that the first principal component has the largest variance. To analyze imbalances, these were used as variables and the individual tumors as the observations; this groups imbalances frequently seen in the same tumors. The obtained factor models were evaluated at two levels, total variance accounted for by the factor models and the estimated communalities for each imbalance. The fraction of the original variance accounted for by the specific factor model is given by the cumulative percentage of the explained variance for each component in the factor model and thus may vary from 0 to 100%. The communality of a given variable (imbalance) is an estimate of how well the factor model predicts the behavior of this variable. The communality ranges from 0 to 1, where a value of 1.0 indicates full explanation of the variance.

3. Results

3.1. Basic statistics

The distribution of chromosome numbers (CN) was dominated by near-diploid cases (CN = 35 – 57); only 13% of the tumors showed polyploid numbers (CN > 57; Fig. 1a). The distribution of the NIPT in the near-diploid cases was near geometrical, with very few tumors having more than seven changes (Fig. 1b). The polyploid cases showed a bimodal distribution, with one group having 1–7 imbalances (category 1) and a second with 8–18 imbalances (category 2; Fig. 1c). Of the selected 28 imbalances, 18 were seen in more than 10% of tumors (Table 1). However, only 11 of these were frequent in the near-diploid subset of tumors, namely +5q, +7, +12, +16, +17, +20, 1p−, 3p−, 6q−, 8p−, and −14, which thus make up the central core of the changes in RCC (Table 1). To estimate the temporal order of the imbalances, the near-diploid subset of tumors was selected. Tumors with a given imbalance were then retrieved and the NIPT distributions were produced. The averages of the bootstrapped modal values of these NIPT distributions were then calculated and used as measures for the time of occurrence. This analysis revealed +7, +10, and 3p− to be early changes (TO < 3); +5q, 8p−, −14, +17, and −17 to be intermediate (TO = 3 – 5); and the remaining imbalances to be late (TO > 5; Fig. 2). The late imbalances +8q, +20, −4, −13, −17, and −18 showed significant ($P < 0.01$) correlations with grade 3 tumors. In addition, the late imbalances 1p−, −4, −13, −18, and −22 showed significant negative correlations with grade 1 tumors. Gain of chromosome 10 behaved differently by being an early imbalance but showing correlation with grade 3 tumors. Furthermore, the karyotypic complexity was significantly correlated with grade.

3.2. Karyotypic pathways

To make a first approximation of the cytogenetic pathways, a PCA was performed on the near-diploid set of tumors using the imbalances as variables and the cases as observations. This analysis revealed three clusters of imbalances, two consisting of gains and one mainly of losses, the latter also including +1q (Fig. 3a). Loss of 3p and gain of 5q were located at some distance, but closer to the losses. When performing a second PCA, the TO was included as an observation because no temporal component was seen in the first PCA [7]. The first principal component in this analysis separated early and late imbalances. The loadings for each imbalance on the first component showed a good correlation to the previously estimated TO values ($r = 0.957$) and, thus, represents a time axis. The second component separated the early gains from the early losses (Fig. 3b). The analyses thereby identified the two major cytogenetic pathways operating in RCC: the conventional RCC pathway initiated by 3p−; followed by +5q or −14; and subsequently by 8p−, −9, 6q−, and then by further losses; and the papillary pathway initiated by +7; followed by +17; and subsequently by +16, +20, +12, +3q, +2, and +8q, in the given order (Fig. 3b). The three-dimensional representation of the PCA (Figs. 3, c and d) suggested a possible subdivision of the +7 pathway into two routes, one containing +17 and +3q and a second containing +16, +20, +12, and +2, which converged at higher TO values. The estimated communalities in the three-component PCA solution ranged from 0.43 to 0.77, except for +10, which showed a communality of 0.16. By including a fourth component, this value increased to 0.55, a change of 0.39, while the changes in the remaining imbalances were marginal, ranging from less than 0.001 to 0.13. Thus, apart from +10, the behavior of the majority of the imbalances was well characterized by the three-dimensional representation.

Because +7 and 3p− are of major importance in the development of RCC, the associations of these imbalances with the remaining ones were investigated in more detail.

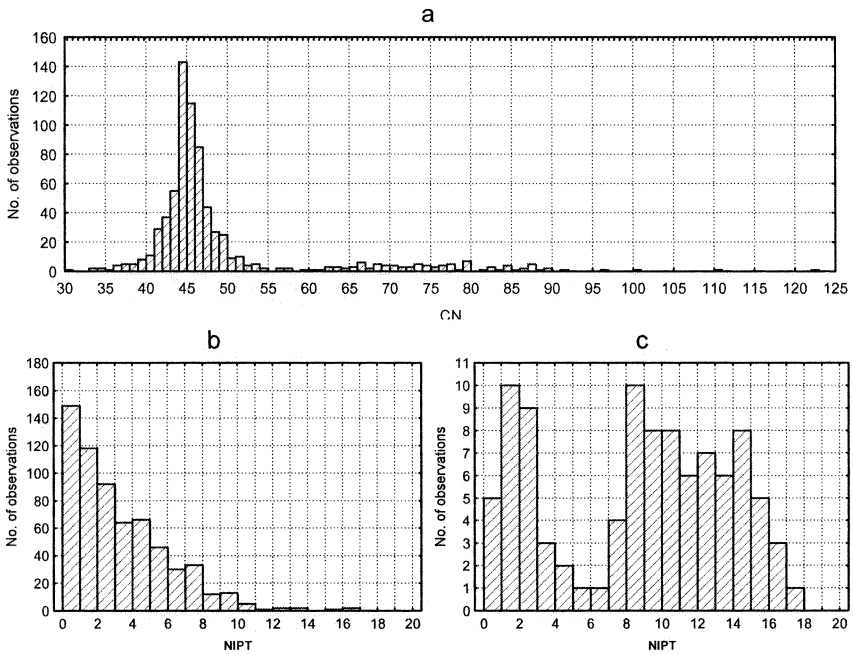

Fig. 1. The distribution of chromosomal changes in RCC. The distribution of (*a*) CN, (*b*) NIPT in near-diploid tumors, and (*c*) NIPT in polyploid tumors.

Table 2 shows that +7 shows significant ($P < 0.01$) associations with 8 of the 12 gains and negative correlation with 6 of the 15 losses, and that 3p− conversely shows negative correlation with 6 of the gains and significant association with 5 of the losses. The strong association between 3p− and +5q is possibly due to the der(3;5), seen in 12% of the cases, that results in the concomitant loss of 3p and gain of 5q.

The near-diploid conventional and papillary carcinomas were then retrieved. Imbalances particularly frequent in the conventional subtype were +5q, +7, 3p−, 8p−, and −14, and those in the papillary subtype were +3q, +7, +12, +16, +17, and +20, all seen in more than 25% of the cases in the respective subtypes (Table 3). Thus conventional carcinomas showed both 3p− and +7 at high frequencies. A PCA of the imbalances present in the conventional carcinomas clearly indicated the presence of both the 3p− and the +7 karyotypic pathways (Fig. 4a). To investigate to what extent the two pathways also were separated in the group of tumors containing both 3p− and +7, tumors with 3p− and +7 were selected and the imbalances were analyzed by MDS. This analysis revealed that even in tumors showing concomitant presence of 3p− and +7, the +7 and the 3p− pathways were well separated (Fig. 4b). The PCA of the imbalances seen in the papillary carcinomas clearly showed the dominating character of the +7 pathway in this subtype (Fig. 4c).

3.3. Polyploid tumors

The polyploid tumors (CN > 57) were divided into category 1 or 2 according to their NIPT values (Fig. 1c) and the frequencies for the respective imbalances were calculated. Category 1 tumors differed from the near-diploid set by showing lower frequencies for the imbalances characteristic for the +7 pathway but comparable frequencies of the 3p− associated imbalances (Table 2). These results suggest that the polyploid tumors with NIPT < 8 primarily originate from hypodiploid tumors (i.e., conventional RCC). The cases with NIPT > 7 were characterized by having high frequencies of all imbalances, including imbalances characteristic for the hyperdiploid pathway, with the possible exception of +10. Both PCA and MDS analyses revealed that the imbalances belonging to the hypo- and the hyperdiploid pathways formed two separate clusters (data not shown). Loss of 1p was seen at significantly ($P < 0.01$) higher frequencies (43%) in polyploid tumors compared with near-diploid ones.

4. Discussion

In the present study, we used the accumulated cytogenetic data from renal cell carcinomas to investigate the karyotypic profiles of conventional and papillary RCC. The chromophobe RCC were too few to allow statistical analyses. By producing genomic imbalance maps, the 28 most common imbalances were identified. After classifying each of the 796 original karyotypes for the presence or absence of these imbalances, 735 had at least one of the selected imbalances. Several statistical methods were then applied to this data set to extract the most important features of the karyotypic evolution.

The distribution of the chromosome numbers was centered on the diploid value, with only a few cases being polyploid. The monotonous nature of the NIPT shows that the investigated material is homogeneous (i.e., no subpeaks

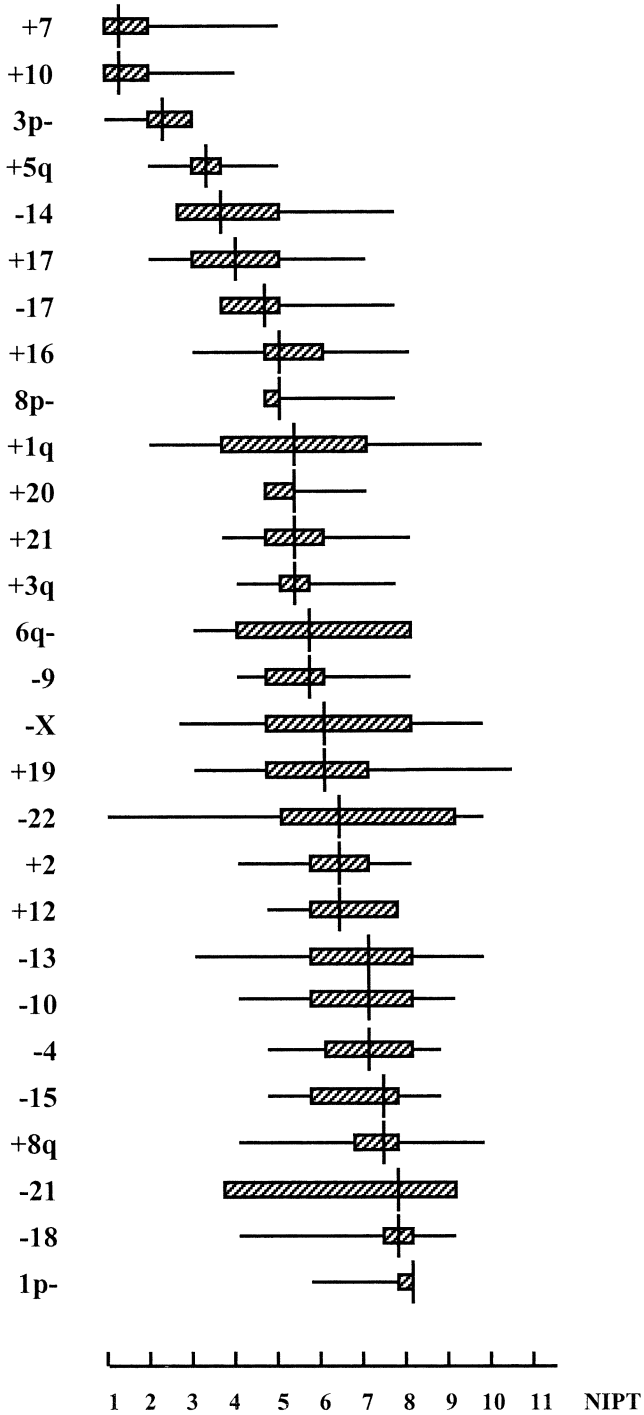

Fig. 2. The temporal analysis of imbalances. Vertical lines in hatched boxes, the mean of the bootstrapped TO; hatched boxes, boundaries of the 25th and 75th percentiles; thin lines, boundaries of the 2.5th and 97.5th percentiles. Imbalances were first sorted according to the TO values, then imbalances with the same TO were organized with respect to the value of the 25th percentile. See Table 1 for abbreviations.

were seen in the distribution). The mono-modal distribution indicates that the mechanism(s) generating chromosomal changes is the same in tumors with simple as in those with complex karyotypes. We have previously shown that the distribution of the number of chromosomal changes in RCC conforms to a power law distribution [11]. Such distributions may reflect that imbalances occur at low frequencies and accumulate over an extended period of time.

We used the modal value of the NIPT distribution of tumors with a given imbalance as a measure for the TO of that imbalance [7]. To obtain a better estimation, the TO was resampled 1000 times and the mean of the bootstrapped TO values used as the final TO. Using this procedure, we have previously derived chronological orders of karyotypic events that correlate with histopathological grading [12–14]. The temporal analysis revealed 3p−, +7, and +10 to be early imbalances; +5q, +17, 8p−, −14, and −17 to be intermediate; and the remaining imbalances to be late (Fig. 2). The determined temporal order of imbalances correlated well with histopathological grade, where early imbalances were predominantly seen in low-grade and the late imbalances in high-grade tumors. Hence, the deduced temporal order of imbalances most likely reflects the order occurring in vivo.

To screen for possible cytogenetic pathways, we reasoned that imbalances frequently present in the same cases should belong to the same tumorigenetic route. Thus, the pattern of correlations among imbalances would reveal possible cytogenetic pathways toward malignancy. To condense the large correlation matrix produced by the 28 imbalances and to extract the central features of the matrix, we performed PCA. The first analysis revealed a strong clustering of gains and of losses, respectively. To obtain a more comprehensive model of the cytogenetic pathways, the PCA was repeated and the TO for each imbalance included as an observation. This organized the imbalances along the first principal component according to the TO values, and by including the second and third components, it was possible to obtain a three-dimensional representation of the cytogenetic pathways [7]. This analysis identified two pathways, one already known to characterize papillary RCC initiated by +7, and one known to characterize conventional RCC initiated by 3p−. Gain of chromosome 7 was followed by +17 and +16 as intermediate imbalances, and then by the remaining gains as late changes. Loss of 3p was followed by +5q, −14, and −17 as intermediate changes, and then by the remaining losses as late changes (Fig. 2). The cytogenetic pathways are summarized in Fig. 5. The early steps in these pathways were very well separated. Gain of chromosome 7 showed negative correlations with most of the important imbalances in the 3p− pathway (e.g., 3p−, −14, and 8p−), and conversely, 3p− showed significant negative associations with many imbalances in the +7 pathway (e.g., +7, +16, and +17). The PCA of the imbalances, however, did suggest that the two pathways converged at later stages.

The PCA of the imbalances in the papillary tumors demonstrated that one pathway, the +7 path, is dominant in this subtype. This conclusion was underscored by the very few (8%) papillary tumors showing 3p−. This latter group may correspond to the class of RCC that shows a papillary growth

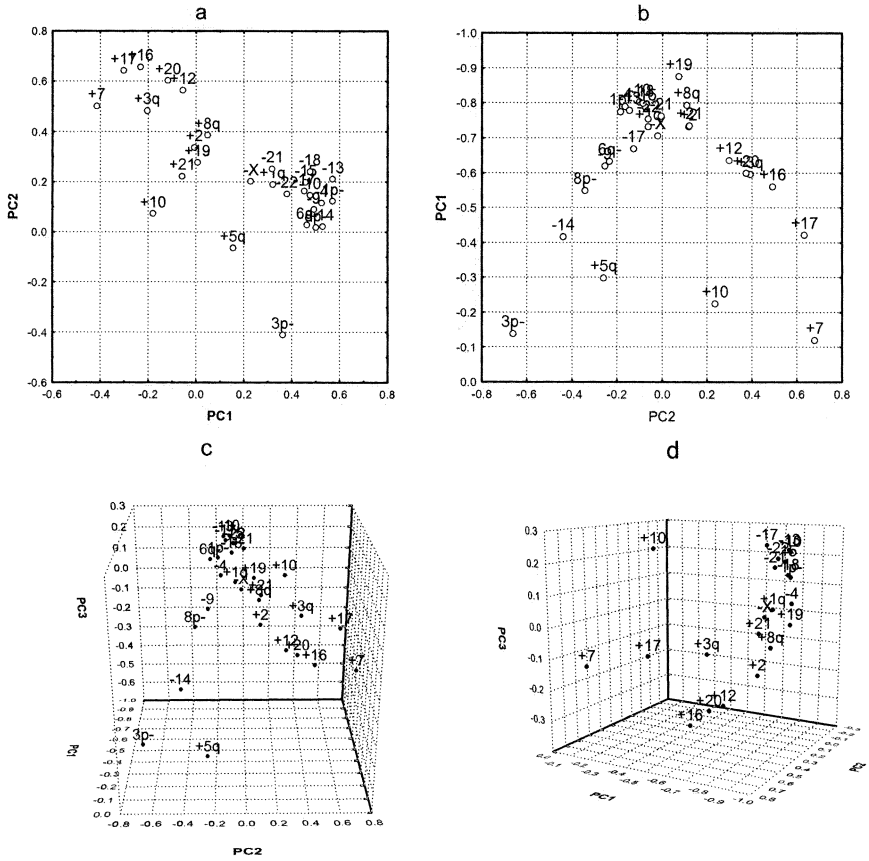

Fig. 3. PCA analysis of the imbalances. (*a*) A two-dimensional representation of the PCA of the imbalances present in the near-diploid tumors; (*b*) a two-dimensional representation of the PCA of the imbalances in the near-diplod tumors when including TO as an observation; (*c*) a three-dimensional representation of the previous PCA; and (*d*) the +7 cytogenetic pathway. To make the +7 pathway more explicit, the imbalances belonging to the 3p− pathway were deleted in Fig. 3d and the figure orientation was changed.

pattern but a cytomorphology characteristic for conventional tumors described by Füzesi and coworkers [15]. In the conventional carcinomas, on the other hand, the corresponding +7, +7, and 3p− classes of tumors were frequent. Furthermore, the PCA of the conventional subtype clearly showed that both the 3p− and the +7 pathways were present as two separate routes. The separation of the pathways was also apparent in the 3p−/+7 class of tumors. Thus, both the 3p− and the +7 pathways are operating in conventional carcinomas, but only the +7 path is operating in the papillary carcinomas (Fig. 5). Nonetheless, only a minority of the conventional tumors showed cytogenetic absence of 3p−. The best interpretation of the data is thus that the presence of 3p− results in conventional RCC, after which the tumor may progress either according to the 3p− or to the +7 pathway. Papillary tumors, on the other hand, progress according to the +7 pathway almost exclusively.

Gain of chromosome 10 behaved differently from the other imbalances. First, it did not cluster with the other gains and a fourth principal component was needed to capture the variation of this imbalance, suggesting a partly independent behavior. Second, even though +10 was considered an early event (TO = 1.7), the presence of this imbalance was correlated with high-grade tumors. As +10 was mostly seen together with imbalances characteristic for the +7 pathway, +10 might contribute a more aggressive behavior to tumors belonging to the hyperdiploid pathway, thus constituting a possible cytogenetic subtype of RCC [16].

Jiang and coworkers [17] suggested the presence of two subtypes of conventional carcinomas, one characterized by 6q−, +17q, and +17p, and one by −9, 13q−, and 18q−. In our study, however, 6q− showed significant ($P = 0.01$) associations with eight losses but with no gains, including +17 (the equivalent of +17q and +17p in Jiang et al. [17]). Gain of chromosome 17 showed significant associations with five gains but not with any loss. Thus, no specific links could be found between 6q− and +17 in the present investigation. Even though −9, −13, and 18q− showed significant associations with each other, these associations were not specific and not different in nature from the associations with other imbalances. Hence, our data do not corroborate the two suggested cytogenetic subtypes. The differences in the detected association patterns, however, could be caused by the fact that Jiang et al. [17] analyzed uncultured material

Table 2
Correlation between 3p− and +7, and the remaining imbalances

Imbalances[a]	+7	3p−
+1q	−0.05	0.04
+2	**0.13**	0.00
+3q	**0.26**	**−0.21**
+5q	−0.08	**0.36**
+7	—	**−0.40**
+8q	**0.13**	−0.07
+10	0.08	**−0.21**
+12	**0.28**	−0.07
+16	**0.30**	**−0.19**
+17	**0.34**	**−0.39**
+19	**0.11**	0.00
+20	**0.27**	**−0.11**
+21	0.08	−0.06
1p−	**−0.12**	0.05
3p−	**−0.40**	—
−4	−0.10	**0.13**
6q−	**−0.18**	**0.14**
8p−	**−0.13**	**0.21**
−9	−0.10	**0.16**
−10	**−0.12**	0.01
−13	−0.10	0.06
−14	**−0.19**	**0.32**
−15	−0.10	−0.04
−17	−0.07	−0.01
−18	−0.06	0.01
−21	−0.04	−0.08
−22	−0.07	−0.08
−X	−0.04	0.08

Boldface represent significant ($P < 0.01$) correlations.
[a] For abbreviations, see Table 1.

Table 3
Frequencies of imbalances in near- diploid conventional and papillary carcinomas

Imbalances[a]	CC ($n = 230$)	Pap ($n = 92$)
+1q	7	10
+2	9	10
+3q	5	30
+5q	41[b,**]	2
+7	30	68
+8q	6	10
+10	5	10
+12	15	29
+16	11	46
+17	6	67
+19	3	11
+20	10	30
+21	3	8
1p−	12*	10*
3p−	80**	9
−4	11	8
6q−	15*	7**
8p−	27	9
−9	23	12
−10	6**	7**
−13	9	8
−14	45	17
−15	7	11
−17	10	7
−18	8	10
−21	3	11
−22	4	10
−X	8	7

Frequencies in percent.
Abbreviations: CC, conventional carcinomas; Pap, papillary carcinomas.
[a] For abbreviations, see Table 1.
[b] Frequencies compared by means of χ^2-test
* $P < 0.05$; ** $P < 0.01$.

by comparative genomic hybridization whereas all cytogenetic investigations involve at least short-term culturing of cells. The analysis of the +7 pathway did, however, reveal substructures: +17 and +3q were located at some distance from the major bulk of the imbalances in this pathway. Jiang et al. [17] have shown that of the two papillary subtypes 1 and 2, first described by Delahunt and Eble [18], type 1 is characterized by +7 and +17. The present data corroborate the existence of such a cytogenetic subtype and, furthermore, suggest that this subtype is also characterized by the presence of +3q as a late imbalance.

Close to 13% of the RCC showed polyploid chromosome numbers. The NIPT distribution of these tumors clearly distinguished two categories, a first category (category 1) with one to seven imbalances and a second (category 2) with more than seven imbalances. The first category showed significantly lower frequencies of imbalances characteristic of the +7 (hypodiploid) than that of the 3p− (hyperdiploid) pathway. If the acquisition of imbalances precedes the polyploidization step, which we find reasonable to assume, the high frequencies of +5q, 1p−, 3p−, 6q−, 8p−, −14, and −17 suggest that hypodiploid cases are more prone to undergo polyploidization than hyperdiploid tumors. Furthermore, because the frequencies of the imbalances as well as the numbers of imbalances per tumors were comparable to what was found for the corresponding diploid tumors, the first polyploid category may represent hypodiploid tumors that have undergone a polyploidization step without any further changes. Loss of 1p may be of particular importance for this step because 1p− was seen at significantly higher frequencies in the polyploid subpopulation.

The second category was characterized by having 8–18 imbalances. This is well above the number of imbalances typically seen in the diploid tumors. As a result, in combination with the polyploidization step, these stages have acquired a large number of additional imbalances. This suggests that the category 2 cases have acquired an increased chromosomal instability not seen in the category 1 tumors. An alternative but less attractive interpretation could be that all tumors with more than eight imbalances go through a polyploidization step. The category 2 cases differed from category 1 cases by showing high frequencies of all imbalances, with the exception of +10. The subsequent PCA and MDS analyses of the imbalances showed that gains and losses were separated in the category 2 cases. This indicates that cells belonging to both pathways may undergo polyploidization, albeit at late stages (Fig. 5).

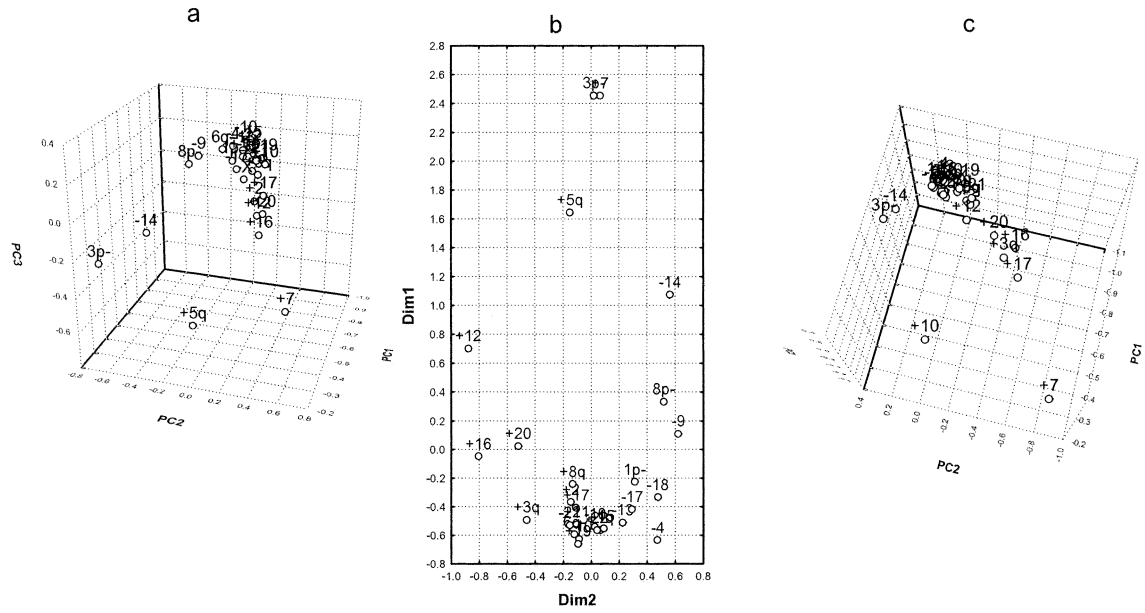

Fig. 4. Analyses of imbalances present in histopathologic subtypes of RCC. (*a*) PCA of imbalances in conventional carcinomas; (*b*) MDS of the imbalances present in cases belonging to the 3p−/+7 subgroup of conventional carcinomas; and (*c*) PCA of imbalances present in papillary RCC.

We recently analyzed lung [19], ovarian [20], and head and neck [21] carcinomas using a similar approach as in the present investigation. In these tumor types, the karyotypic evolution demonstrated three distinct phases, I, II, and III. The near-diploid phase I cases typically contained one to seven imbalances and showed a near-geometrical NIPT distribution, very similar to the one obtained for RCC. In addition, the near-diploid phase I lung and ovarian tumors showed distinct cytogenetic pathways. The near-diploid RCC are thus similar to the near-diploid lung and ovarian phase I tumors. On the other hand, the phase II tumors seen in ovarian and lung carcinoma are near-diploid but have 8–16 imbalances and show a less distinct karyotypic pattern [19,20]. This category is not seen in RCC. In ovarian carcinoma we were able to show that the presence of internuclear bridges, an indicator for the occurrence of chromosome instability though breakage–fusion–bridge (BFB) cycles, was correlated with phase II tumors [20]. The absence of phase II in near-diploid RCC tumors may thus indicate that BFB cycles are not frequent in this tumor type, even though phenomena similar to telomere crises have been described [22]. In fact, recent investigations have shown that BFB cycles are rare in RCC and appear to be confined to tumors with polyploid clones (Gisselsson D, unpublished results). Taken together, the data suggest that only two phases of karyotypic evolution are seen in RCC, whereas three may be distinguished in lung and ovarian carcinoma. This would indicate that the propensity for chromosomal instability is relatively low in conventional and papillary RCC [23] compared with these neoplasms.

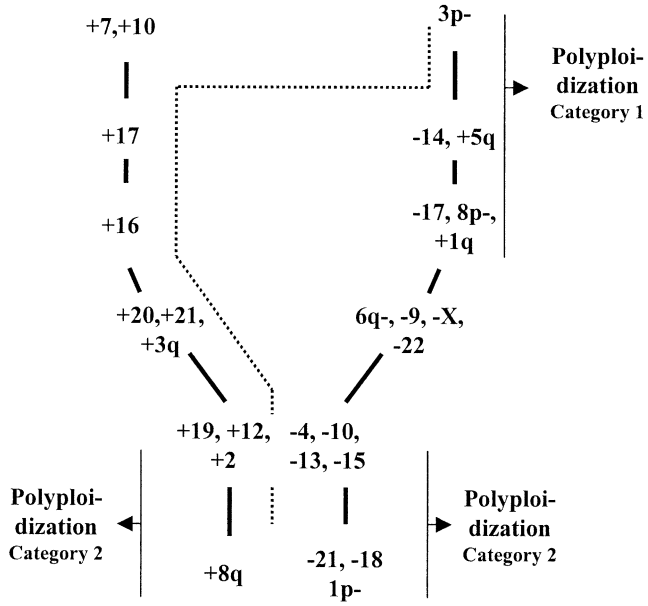

Fig. 5. A summary of the cytogenetic pathways in RCC. *Thick line*, the major cytogenetic pathways in RCC; *dotted line*, the alternative minor route seen in conventional RCC.

Acknowledgments

This work was supported by the Swedish Cancer Society, the Crafoord Foundation, and the Nilsson Family Foundation.

References

[1] Kovacs G. Molecular cytogenetics of renal cell tumours. Adv Cancer Res 1993;62:89–124.

[2] Kovacs G, Akhtar M, Beckwith BJ, Bugert P, Cooper CS, Delahunt B, Eble JN, Fleming S, Ljungberg B, Medeiros LJ, Moch H, Reuter VE, Ritz E, Roos G, Schmidt D, Srigley JR, Storkel S, van den Berg E, Zbar B. The Heidelberg classification of renal cell tumours. J Pathol 1997;183:131–3.

[3] van den Berg E, Dijkhuizen T, Oosterhuis JW, Geurts van Kessel A, de Jong B, Storkel S. Cytogenetic classification of renal cell cancer. Cancer Genet Cytogenet 1997;95:103–7.

[4] Kovacs G, Füzessi L, Emanual A, Kung HF. Cytogenetics of papillary renal cell tumours. Genes Chromosomes Cancer 1991;3:249–55.

[5] Speicher MR, Schoell B, du Manoir S, Schrock E, Ried T, Cremer T, Storkel S, Kovacs A, Kovacs G. Specific loss of chromosomes 1, 2, 6, 10, 13, 17, and 21 in chromophobe renal cell carcinomas revealed by comparative genomic hybridization. Am J Pathol 1994;145:356–64.

[6] Mitelman database of chromosome aberrations in cancer. Mitelman F, Johansson B, Mertens F, editors. Available at: http://www.cgap.nci.nih.gov/Chromosomes/Mitelman. Accessed November 2002.

[7] Höglund M, Gisselsson D, Säll T, Mitelman F. Coping with complexity. Multivariate analysis of tumor karyotypes. Cancer Genet Cytogenet 2002;135:103–9.

[8] Mooney CZ, Duval RD. Bootstrapping: a nonparametric approach to statistical inference. Sage University Paper Series on Quantitative Applications in the Social Sciences, series no. 07–095. Thousand Oaks, CA: Sage, 1993.

[9] Kachigan SK. Statistical analysis. New York: Radius Press, 1996.

[10] Affifi A, Azen S, editors. Statistical analysis. A computer oriented approach. New York: Academic Press, 1979, pp. 318–24.

[11] Frigyesi A, Gisselsson D, Mitelman F, Höglund M. Power law distribution of chromosome aberrations in cancer. Cancer Res 2003;63:7094–7.

[12] Höglund M, Säll T, Heim S, Mitelman F, Mandahl N, Fadl-Elmula I. Identification of cytogenetic subgroups and karyotypic pathways in transitional cell carcinoma. Cancer Res 2001;61:8241–6.

[13] Höglund M, Gisselsson D, Hansen GB, Säll T, Mitelman F. Multivariate analysis of chromosomal imbalances in breast cancer delineates cytogenetic pathways and reveals complex relationships among imbalances. Cancer Res 2002;62:2675–80.

[14] Höglund M, Gisselsson D, Hansen GB, Säll T, Mitelman F, Nilbert M. Dissecting karyotypic patterns in colorectal tumours: two distinct but overlapping pathways in the adenoma-carcinoma transition. Cancer Res 2002;62:5939–46.

[15] Füzesi L, Gunawan B, Bergman F, Tack S, Braun S, Jakse G. Papillary renal cell carcinoma with conventional cytomorphology and chromosomal loss of 3p. Histopathology 1999;35:157–61.

[16] Meloni A, Pontes JE, Sandberg AA. Trisomy 10 in renal cell carcinoma. Cancer Genet Cytogenet 1991;51:137–8.

[17] Jiang F, Richter J, Schraml P, Bubendorf L, Gasser T, Sauter G, Mihatsch MJ, Moch H. Chromosomal imbalances in papillary renal cell carcinoma: genetic differences between histological subtypes. Am J Pathol 1998;153:1467–73.

[18] Delahunt B, Eble J. Papillary renal cell carcinoma: a clinicopathologic and immunohistochemical study of 105 tumours. Mod Pathol 1997;10:537–44.

[19] Höglund M, Gisselsson D, Hansen GB, Mitelman F. Statistical dissection of cytogenetic patterns in lung cancer reveals multiple modes of karyotypic evolution independent of histological classification. Cancer Genet Cytogenet (in press).

[20] Höglund M, Gisselsson D, Hansen GB, Säll T, Mitelman F. Ovarian carcinoma develops through multiple modes of chromosomal evolution. Cancer Res 2003;63:3378–85.

[21] Höglund M, Jin C, Gisselsson D, Hansen GB, Mitelman F, Mertens F. Statistical analyses of karyotypic complexity in head and neck squamous cell carcinoma. Cancer Genet Cytogenet 2004;150:1–8.

[22] Holzmann K, Blin N, Welter C, Zang KD, Seitz G, Henn W. Telomeric associations and loss of telomeric DNA repeats in renal tumours. Genes Chromosomes Cancer 1993;6:178–81.

[23] Contractor H, Zariwala M, Bugert P, Zeisler J, Kovacs G. Mutation of the p53 tumour suppressor gene occurs preferentially in the chromophobe type of renal cell tumour. J Pathol 1997;181:136–9.